

# Miniaturization of MALDI Mass Spectrometers with the Technological Breakthrough of the Digital Ion Trap: Peptide and Protein Analysis in MS<sup>1</sup>, MS<sup>2</sup>, and MS<sup>3</sup>

Andreas Baumeister<sup>a,\*</sup>, Lyna Sellami<sup>a</sup>, and Shuichi Nakaya<sup>b</sup>

**Abstract:** A digital ion trap (DIT) mass spectrometer was developed to extend the mass range in comparison to conventional ion traps. This was achieved by changing the RF voltage from a sinusoidal to a rectangular waveform. In addition to the extended mass range, the size of the instrument was miniaturized. To show the benefits of this development, MALDI applications in MS<sup>1</sup>, MS<sup>2</sup>, and MS<sup>3</sup> are presented: On one hand, it is possible to analyze intact proteins, on the other hand the instrument enables insights into the structure of antibodies and glycoproteins after enzymatic digestion and collision-induced dissociation (CID).

**Keywords:** Digital ion trap · Glycopeptide · MALDI · Miniaturization · MS<sup>3</sup>



**Andreas Baumeister** received his BSc in chemistry and physics and his MSc in business chemistry at Münster University in Germany. He worked in Klaus Dreisewerd's lab and obtained his PhD in analytical chemistry. His research aimed to gain deeper insights into the MALDI process. Therefore, he performed studies on the wavelength dependency of the MALDI process and developed a surface-assisted

LDI method for crude lipid mixtures based on etched silver foil. Since 2018, he has been working in the European headquarters of Shimadzu as an application specialist for the MALDI product line. He is responsible for application support and representation of Shimadzu and their products at international events.



**Lyna Sellami** received her BSc in Engineering for health and medications at Grenoble's faculty of pharmacy (France) then obtained her PhD in proteomics applied to human pathologies at Aix-Marseille University (France) in 2013. Her research aimed to gain deeper insight into the oxidative stress process using mainly MALDI mass spectrometry; she also developed and patented an analytical method

for the characterization of oxidative post-translational modifications. After her PhD, she worked as an applications specialist in MALDI mass spectrometry in the UK then in Germany where she currently works in the Center of Innovation and Product Support of Shimadzu European Headquarters.



**Shuichi Nakaya** holds a master's degree in integrated biosciences from the University of Tokyo. He participated in the Japanese Glycomics Project from 2003 to 2006 and was involved in the development of a glycan structure analysis system using mass spectrometry. He works as an application chemist at Shimadzu Corporation and mainly performs various analyses using mass spectrometry.

## 1. Introduction

Matrix-Assisted Laser Desorption Ionization (MALDI) mass spectrometry is a soft ionization technique for molecular analysis of purified molecules<sup>[1]</sup> as well as complex samples such as cells<sup>[2]</sup> and tissues.<sup>[3]</sup> It is fast, robust, and requires minimal sample preparation thanks to its tolerance to many impurities.<sup>[4]</sup> The first commercially available MALDI-MS systems were released in the early nineties with typical dimensions of two meters in length. Over the years, less bulky MALDI mass spectrometers began to emerge with the advent of miniaturized components and advancements in electronics making field applications more feasible. Nevertheless, MALDI time of flight (TOF) instruments still occupy large laboratory space with relatively high power consumption and associated costs. It remains desirable to have MALDI instruments downsized whilst keeping the same performance. Most quadrupole ion traps that are based on an electric field driven by a radiofrequency (RF) generated sinusoidal wave voltage present a restricted upper limit of the mass range.<sup>[5]</sup> Several technological improvements allowed for the release of benchtop MALDI-TOF instruments. However, they lack the capability of performing MS<sup>2</sup> and MS<sup>3</sup> fragmentation.

In this article, we introduce the technological breakthrough of the digital ion trap (DIT) which is capable of overcoming the challenge of keeping good performance whilst downsizing the MALDI instrument. The DIT uses a rectangular wave RF rather than the conventional sinusoidal wave RF. The voltage amplitude of the DIT is lowered to 1 kV.<sup>[6,7]</sup> This allows, firstly, to analyze a higher mass range compared to conventional ion traps and, secondly, to reduce significantly instrument dimensions. Hence, this

\*Correspondence: Dr. A. Baumeister, E-mail: abm@shimadzu.eu

<sup>a</sup>Center of Innovation and Product Support, Shimadzu Europa GmbH, Duisburg, Germany; <sup>b</sup>Solutions Center of Excellence, Shimadzu Corporation, Kyoto, Japan

DIT could be an alternative to a TOF system for the sake of device miniaturization.<sup>[8,9]</sup>

In this article, we present the MALDImini-1, the smallest MALDI instrument having a footprint of an A3 paper size and a total instrument volume below 40 L. We explain how this instrument is capable of analyzing a broad mass range in the MS mode and performing MS<sup>2</sup> and MS<sup>3</sup> analysis using protein and peptide samples.

### 1.1 MALDI-DIT Instrument Overview

The MALDI-DIT mass spectrometry instrument called MALDImini<sup>TM</sup>-1 was developed by Shimadzu Corporation, Kyoto, Japan.<sup>[8]</sup> It is the smallest MALDI-MS system with the dimensions of 31 (W) × 39 (D) × 32 (H) cm and a weight of 25 kg (Fig. 1A). Inside the housing are fitted the sample loading system with a capacity of 48 samples, an Nd:YLF laser (wavelength of 349 nm), the three-dimensional quadrupole digital ion trap (3D-QIT), the detector, and the vacuum system consisting of a diaphragm pump and a turbo molecular pump.

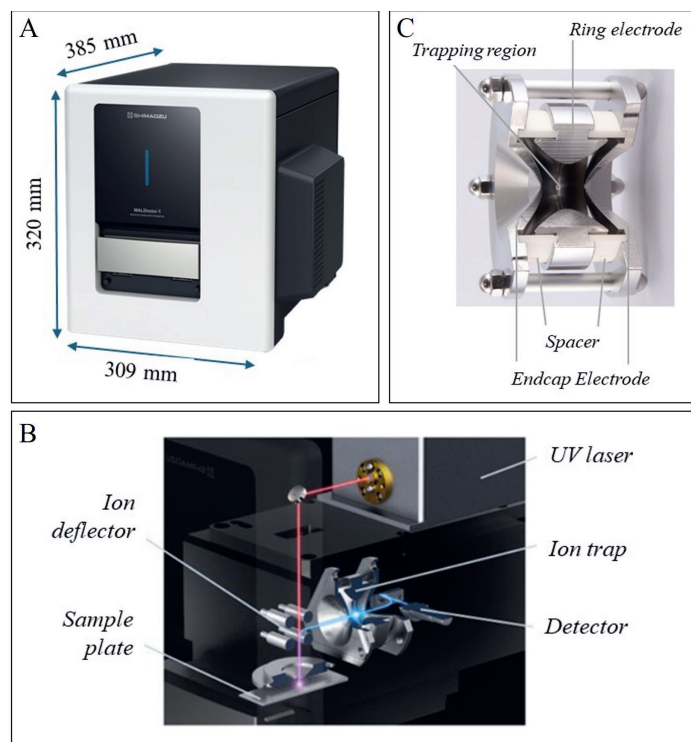


Fig. 1. MALDImini-1 DIT mass spectrometer from Shimadzu. A) Exterior, B) internal component configuration, C) photo of quarter 3D-QIT.

The key features of the instrument are the high mass range provided by the digital ion trap in combination with the MS<sup>3</sup> capability and the small footprint: The operating mass range of the instrument is  $m/z$  650–70,000 in the MS mode and  $m/z$  350–5,000 in the MS<sup>n</sup> mode. The instrument runs in the positive ion mode with a resolution above 4,000 for peptides at  $m/z$  1,500. Helium is required for the analysis as a cooling gas and argon as a collision gas for CID experiments.

The principles of sample measurement are as follows:

1. **Ionization:** The system is equipped with a MALDI source and undergoes the regular desorption process. Briefly, when the samples-matrix mixture is irradiated with a pulsed UV laser, the sample is desorbed and ionized in the gas phase.<sup>[10]</sup>

2. **Ion trapping:** The generated ions are extracted by an electric field and deflected by 90° in a quadrupole deflector (Fig. 1B). Ions are then introduced into the ion trap and cooled down using helium gas, reducing their kinetic energy.

3. **Mass scanning:** By decreasing the frequency of the rectangular voltage applied to the ring electrode and simultaneously exciting ions by dipole excitation, ions are ejected from the ion trap in an ascending  $m/z$  order. Ejected ions collide with a conversion dynode electrode and generate secondary electrons, which are converted to electrical signals in the detector and recorded. The recorded data are processed by the software and then displayed as a mass spectrum.

4. **MS<sup>2</sup> and MS<sup>3</sup> modes:** Precursor ions with targeted  $m/z$  values are isolated in the ion trap by digital asymmetric wave isolation (DAWI). This is explained in the section ‘Digital Ion Trap Technology’ of this article.

## 2. Digital Ion Trap Technology

### 2.1 DIT vs. Conventional Ion Traps

An ion trap is a device for trapping ions in a particular region formed by an electric or magnetic field in a vacuum.<sup>[11]</sup> It can perform several operations, such as trapping ions, ejecting them in an increasing order of  $m/z$ , and isolating targeted ions for fragmentation to provide structural information.<sup>[11]</sup> RF traps use an electric field. They are constituted of two end caps and a ring electrode<sup>[12]</sup> to which direct current (DC) and RF generated sinusoidal wave voltages are applied. They are smaller in size and easier to operate than magnetic field ion traps.

MALDI-MS analysis predominantly generates singly charged ions and requires a broad mass range. However, most quadrupole ion traps have a limited upper mass range because mass scans require changing the RF voltage to some tens of kilovolts in amplitude. This is technically challenging due to overheating.<sup>[5,13]</sup>

The new digital ion trap uses a rectangular wave RF rather than the conventional sinusoidal wave RF, with timings that are controlled by high-precision digital circuits which precisely control the frequency and the modulation of the digital waveform.<sup>[6]</sup> During a mass scan, the frequency is scanned instead of the amplitude (Fig. 2A).<sup>[7]</sup> Switching voltages provide the trapping electric field.

In fact, there is no need for inevitably large-scale components that are inherent to high voltage power source requirements over 10 kV. The smaller volume occupied by the smaller components leads to a reduction in the instrument footprint and power consumption. The DIT could substitute the TOF for the sake of miniaturization of the device.<sup>[8,9]</sup> Thus, compared to conventional ion traps, the DIT can analyze a higher mass range up to 70 kDa.

### 2.2 The DIT for MS and MS<sup>n</sup> Analysis

The functionality of the DIT is described in detail by Iwamoto *et al.*<sup>[9]</sup> In summary, the rectangular voltage is applied to the ring electrode. It consists of a direct current component  $U$  and an alternating current component  $V$  with a rectangular wave. In normal operation,  $V_1$  and  $V_2$  of the rectangular voltage have the same amplitude but opposite polarity. The duty ratio between the high voltage  $V_1$  and low voltage  $V_2$  is  $d = 0.5$ .

Based on these values, the *Mathieu equation* determines the stability region for the DIT in the same manner as for an RF trap with a sinusoidal voltage. Trapped ions are ejected in an order of increasing  $m/z$  to the detector (Fig. 2B). Theoretically, with this setup there is no upper limit for the  $m/z$  of ions but there is a low mass cutoff value for  $m/z$  corresponding to  $q_0 = 0.7125$ .

A simulation of the ion trapping and ejection in the DIT was conducted by Ding *et al.*<sup>[6]</sup> The trajectory amplitudes of the ions are an asymmetric waveform in contrast to harmonic oscillation for conventional ion traps. The calculated mass resolution was 6,200 for an ion with  $m/z$  of 1,750 and a scan rate of approx. 4,000 Th/s. In fact, the measured resolution is above 4,000 with this scan rate for a peptide with slightly lower  $m/z$ . A similar resolution can be achieved with a conventional quadrupole ion

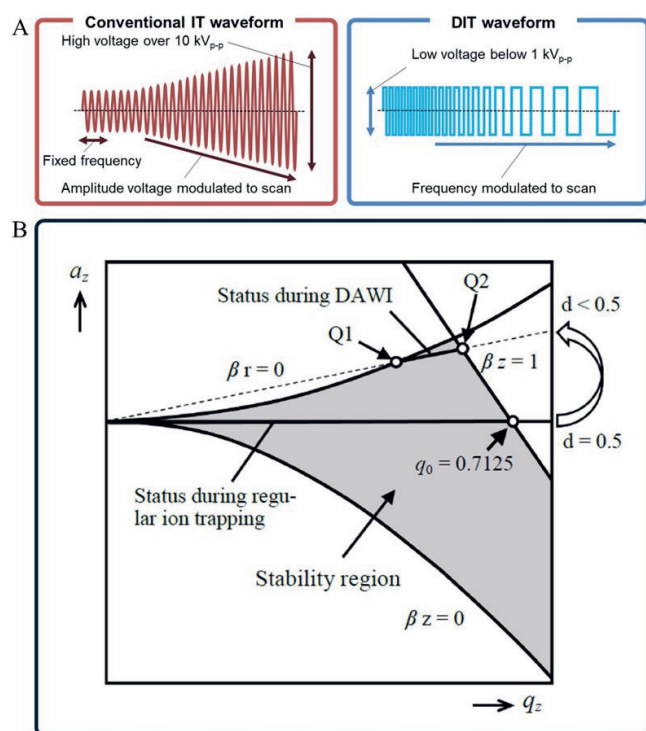


Fig. 2. A) Comparison of a conventional ion trap waveform and a digital ion trap waveform. B) Stability region of the DIT.

trap but with a limited mass range.<sup>[14]</sup> The simulation study<sup>[6]</sup> also showed that the voltage amplitude of the DIT that is needed can be lowered to about 1 kV.

For  $MS^n$  modes, the MALDImini-1 implements a unique and highly efficient precursor isolation technique using Digital Asymmetric Wave Isolation (DAWI). It is achieved by changing the duty ratio of the rectangular voltage waveform to a value lower than 0.5. The mass scan line in the  $a_z$ - $q_z$ -plane becomes sloped as indicated by the dashed line in Fig. 2B. The ions in the specific mass range between intersection points Q1 and Q2 can remain in the trap and all other ions are ejected. DAWI efficiently isolates precursor ions within milliseconds by using the boundary ejection to exclude ions. In the MALDImini-1,  $m/z$  selectivity for precursor isolation is improved by repeating DAWI twice at different frequencies.

In the  $MS^2$  mode, a product ion mass spectrum is acquired by mass scanning after applying CID. For  $MS^3$ , targeted CID fragments are isolated by DAWI and fragmented further by CID before mass scanning.

### 3. Applications

#### 3.1 High Mass Range

The first example illustrates the high mass range analysis capabilities of the MALDImini-1. The spectrum (Fig. 3A) shows the singly charged, doubly charged, and triply charged ions of the *bovine serum albumin* (BSA) protein. Compared to MALDI-TOF measurements of the same preparation, multiply charged ions are more represented than the singly charged ions.

This difference could be explained by the fact that ions are ejected in an ascending order (see section 2.2): Higher  $m/z$  ions are stored for a longer time in the ion trap than smaller  $m/z$  ions. With increasing storage time, the metastable decay<sup>[15]</sup> leads to an increased fragmentation rate and a lesser amount of intact singly charged ions can be detected.

#### 3.2 Peptide Sensitivity

The second example (Fig. 3B) shows the sensitivity of the system using Glu1Fibrinopeptide (GluFib) where 50 amol was

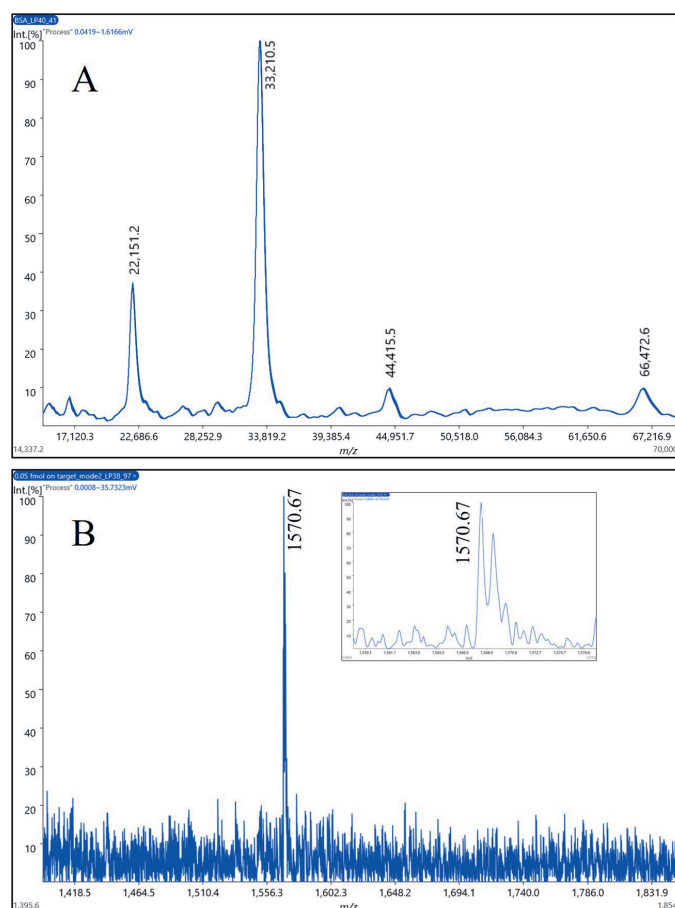


Fig. 3. A) 2.5 pmol of bovine serum albumin on the target: The target was precoated with sinapinic acid matrix solution and the remaining solution was removed after 10 s. Afterwards, 0.5  $\mu$ L of BSA solution (5 pmol/ $\mu$ L) and 0.5  $\mu$ L of matrix solution were added to the precoated area. B) 50 amol of Glu1-Fibrinopeptide B on the target: 0.1  $\mu$ L each of CHCA solution and GluFib solution (500 amol/ $\mu$ L) were applied to the target.

detected. This ultimate sensitivity was achieved using a hydrophilic/hydrophobic modified surface of the stainless steel target, allowing us to concentrate the peptide on a smaller surface.<sup>[16,17]</sup>

The peptide sensitivity specification on the MALDImini-1 is 1 fmol on target. Consequently, the modification of the surface of the target allowed for an increase in the sensitivity of detection by a factor of 20.

#### 3.3 Determination of Modification Site on a Chemically Modified Antibody

The third illustration is an example that mimics the characterization process of antibody drug conjugates, where it is crucial to identify the cytotoxic drug binding site to the antibody in order to assess its efficacy and safety. Briefly, a standard antibody (NIST-mab, humanized IgG K monoclonal antibody, RM8671) was modified with Me-fluorescein-ABNO on a tryptophan residue, as described by Seki *et al.*<sup>[18]</sup> For comparison, the non-modified antibody was analyzed. This application is further described by Iwamoto *et al.*<sup>[9]</sup>

The  $MS^1$  spectrum of the trypsin digested modified antibody showed (Fig. 4) several species that were only detected in the modified antibody sample, such as  $m/z$  2416.9 that was selected for  $MS^2$  analysis (Fig. 5A).

The  $MS^2$  spectrum of  $m/z$  2416.9 is dominated by the fragments corresponding to the peptide backbone after the neutral loss of the Me-fluorescein-ABNO modification. The species at  $m/z$  1677.7 was then selected for  $MS^3$  analysis (Fig. 5B). It showed

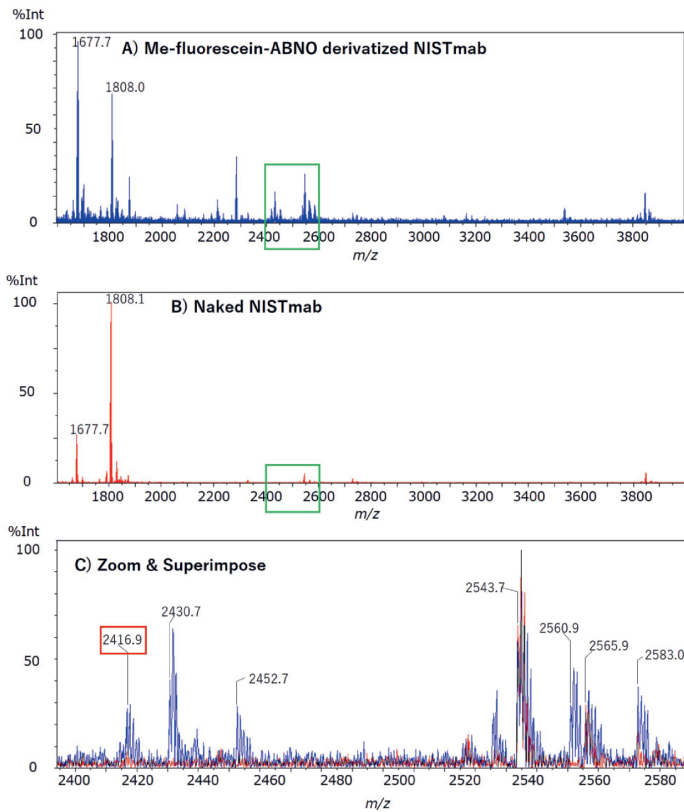


Fig. 4. MS<sup>1</sup> spectra comparison of A) digest of the modified antibody, B) digest of the naked antibody, and C) zoom and overlay of A) and B). Both samples were digested by trypsin and desalted with a ZipTip® µC18 tip. Samples were prepared with 2,5-dihydroxybenzoic acid (DHB) using the dried droplet method, modified from ref. [9].

the same fragment pattern as the MS<sup>2</sup> spectrum of a same species at  $m/z$  1677.7 found in the MS<sup>1</sup> spectrum of the native antibody (Fig. 5C). The data confirm that the antibody was modified at that part of the sequence.

Finally, a Mascot MS/MS ion search confirmed the peptide sequence FNWYVDGVEVHNAK (Fig. 5D) and showed that the fragments corresponded to y- and b-ions of the peptide. Since the Me-fluorescein-ABNO modification is specific to tryptophan residues, it can be concluded that the binding site was identified.

A similar strategy for sequence confirmation with a MALDI-DIT instrument was already demonstrated by Shu *et al.*[19] to distinguish different ebolavirus species by analyzing tryptic peptides of viral matrix proteins.

### 3.4 Analysis of Glycopeptides

Glycoproteins and glycopeptides are molecules with structural heterogeneity formed by the bonding of glucose, mannose, and other monosaccharides. Elucidating glycoprotein structures is essential for uncovering their roles in biological processes such as cell signaling and for the development of biopharmaceuticals.[20]

To demonstrate the instrument's capability for glycoprotein analysis, a commercial monoclonal antibody was reduced, alkylated and trypsin digested. The glycopeptide fraction was then separated by a pipette tip packed with Sepharose CL4B.[21]

Fig. 6 shows the MS<sup>1</sup> spectrum of the glycopeptide fraction. In total, 8 different species were observed that showed typical mass differences for common monosaccharides.

The MS<sup>2</sup> analysis (Fig. 7A) of the ion at  $m/z$  2796.2 shows the glycan-derived product ions. Based on the mass differences, the structure of the sugar chain was identified. A triplet peak having

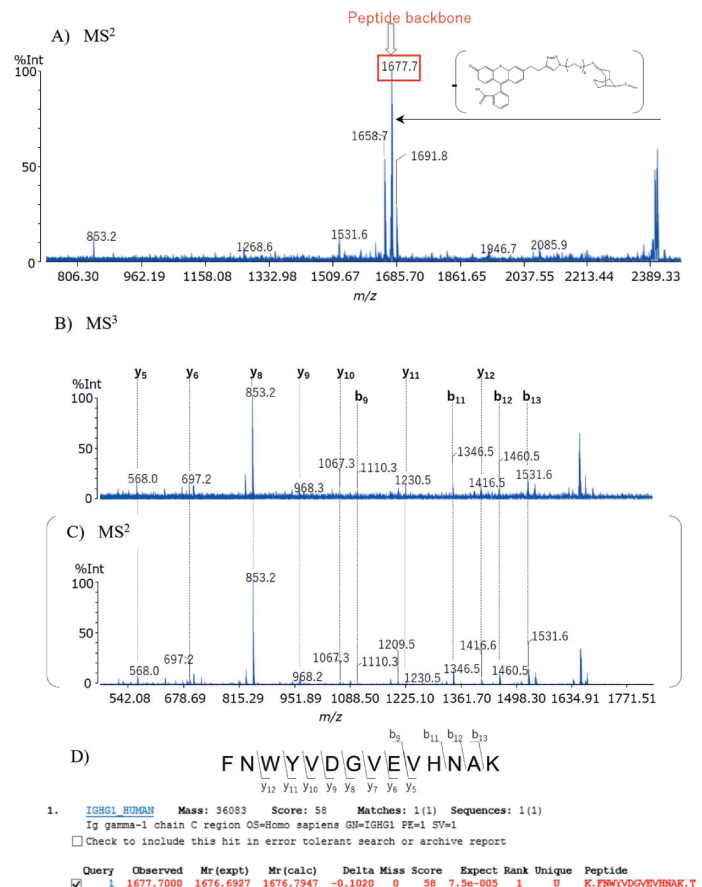


Fig. 5. A) MS<sup>2</sup> and B) MS<sup>3</sup> spectra of the tryptic digest of the modified antibody, and C) MS<sup>2</sup> spectrum of the tryptic digest of the naked antibody for comparison. D) Result of Mascot MS/MS search. Modified from ref. [9].

the distinctive mass differences ( $\Delta m/z$  83, 120) of GlcNAc at the root of *N*-glycan was also detected.

The smallest and second smallest ions of this triplet were selected as precursors for the MS<sup>3</sup> analysis (Fig. 7 B and C). Fig. 7B shows the y-ions of the peptide backbone of the glycopeptide. The spectrum in Fig 7C was generated with a higher precursor mass ( $\Delta m/z$  83). The  $m/z$  of  $y_3$  and  $y_4$  were the same and the  $m/z$

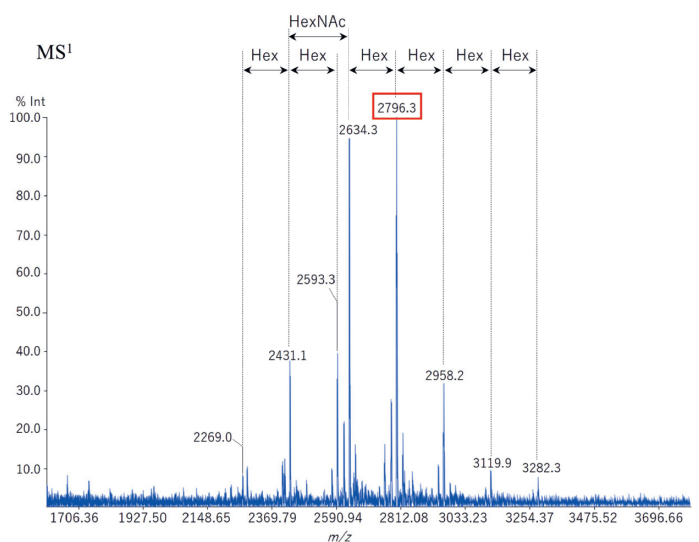


Fig. 6. MS<sup>1</sup> spectrum of the glycopeptide fraction after digest of a monoclonal antibody. Dried droplet preparation with DHB matrix.

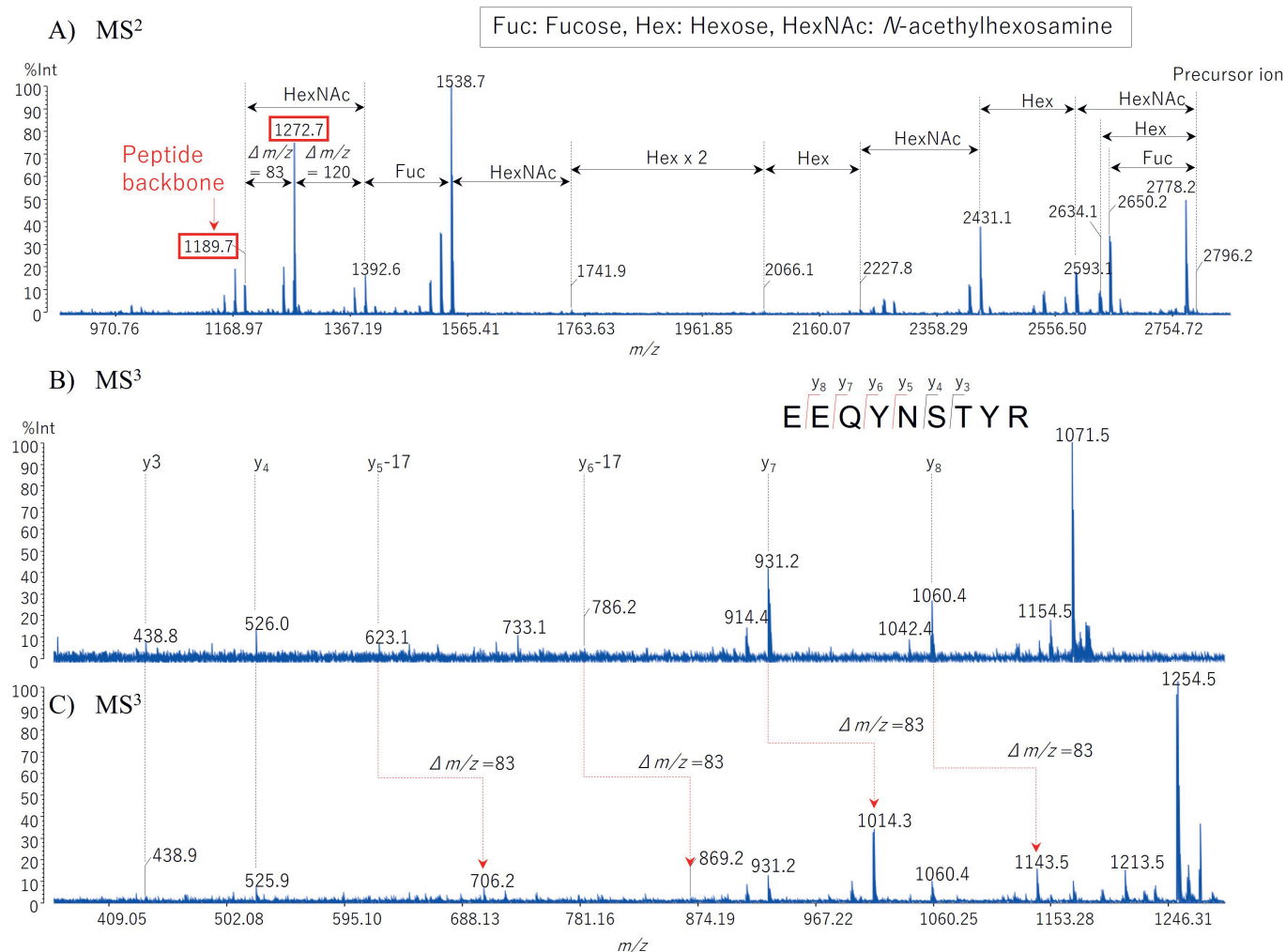


Fig. 7 A) MS<sup>2</sup> spectrum of glycopeptide (precursor ion  $m/z$  2796.2). B) MS<sup>3</sup> spectrum of the peptide backbone (precursor ion  $m/z$  1189.7). C) Peptide backbone containing a partial structure of the Root GlcNAc (precursor ion  $m/z$  1189.7 + 83 = 1272.7).

for  $y_5$  to  $y_8$  were shifted by + 83 Da, confirming that asparagine is the glycan binding site.

#### 4. Conclusions

The development of the MALDImini-1, powered by the DIT technology, represents a transformative step in the field of mass spectrometry. This innovative instrument achieves a remarkable balance between compact design and high analytical performance. The application examples presented in this article underscore the instrument's potential to facilitate biomolecular characterization while addressing the growing demand for smaller, more efficient analytical tools. The unique combination of a broad mass range coupled with MS<sup>3</sup> functionality sets this technology apart.

Future research should focus on further optimizing the DIT technology and exploring its applications in diverse biological and pharmaceutical contexts, ultimately contributing to the evolution of mass spectrometry as an indispensable tool in scientific research.

#### Acknowledgements

We would like to thank the Laboratory of Synthetic Organic Chemistry (Motomu KANAI Group), Graduate School of Pharmaceutical Sciences, The University of Tokyo for preparing the antibody modified with Me-fluorescein-ABNO.

Received: October 30, 2024

- [1] M. Karas, F. Hillenkamp, *Anal. Chem.* **1988**, *60*, 2299, <https://doi.org/10.1021/ac00171a028>.
- [2] J. O. Lay Jr., *Mass Spectrom. Rev.* **2001**, *20*, 172, <https://doi.org/10.1002/mas.10003>.
- [3] D. Gode, D. A. Volmer, *Analyst* **2013**, *138*, 1289, <https://doi.org/10.1039/C2AN36337B>.
- [4] K. Dreisewerd, *Chem. Rev.* **2003**, *103*, 395, <https://doi.org/10.1021/cr010375i>.
- [5] K. W. Lee, G. S. Eakins, M. S. Carlsen, S. A. McLuckey, *J. Am. Soc. Mass Spectrom.* **2019**, *30*, 1126, <https://doi.org/10.1007/s13361-019-02156-z>.
- [6] L. Ding, M. Sudakov, S. Kumashiro, *Int. J. Mass Spectrom.* **2002**, *221*, 117, [https://doi.org/10.1016/S1387-3806\(02\)00921-1](https://doi.org/10.1016/S1387-3806(02)00921-1).
- [7] L. Ding, M. Sudakov, F. L. Brancia, R. Giles, S. Kumashiro, *J. Mass Spectrom.* **2004**, *39*, 471, <https://doi.org/10.1002/jms.637>.
- [8] S. Iwamoto, K. Kodera, S. Sekiya, US Patent US8173961B2, **2008**.
- [9] S. Iwamoto, K. Hosoi, M. Furuta, H. Shichi, S. Yamauchi, T. Nishikaze, S. Nakaya, K. Watanabe, K. Kodera, K. Tanaka, 'Development of MALDImini-1 Digital Ion Trap Mass Spectrometer', *Shimadzu Rev.* **2020**, *77*, [https://www.shimadzu.com/about/magazine/tec\\_news/srv77\\_12/report07.html](https://www.shimadzu.com/about/magazine/tec_news/srv77_12/report07.html).
- [10] M. Karas, D. Bachmann, U. Bahr, F. Hillenkamp, *Int. J. Mass Spectrom. Ion Processes* **1987**, *78*, 53, [https://doi.org/10.1016/0168-1176\(87\)87041-6](https://doi.org/10.1016/0168-1176(87)87041-6).
- [11] J. V. Johnson, R. A. Yost, P. E. Kelly, D. C. Bradford, *Anal. Chem.* **1990**, *62*, 2162, <https://doi.org/10.1021/ac00219a003>.
- [12] W. Paul, H. Steinwedel, US Patent No. US2939952A, **1954**.
- [13] M. Karas, R. Krüger, *Chem. Rev.* **2003**, *103*, 427, <https://doi.org/10.1021/cr010376a>.
- [14] R. W. Smith, in 'Encyclopedia of Forensic Sciences', Ed. M. M. Houck, Elsevier, <https://doi.org/10.1016/B978-0-12-823677-2.00054-4>.
- [15] B. Spengler, D. Kirsch, R. Kaufmann, *Rapid Commun. Mass Spectrom.* **1991**, *5*, 198, <https://doi.org/10.1002/rcm.1290050412>.
- [16] M. Benz, A. Asperger, M. Hamster, A. Welle, S. Heissler, P. A. Levkin, *Nat. Commun.* **2020**, *11*, 5391, <https://doi.org/10.1038/s41467-020-19040-0>.

- [17] M. Benz, M. R. Molla, A. Böser, A. Rosenfeld, P. A. Levkin, *Nat. Commun.* **2019**, *10*, 2879, <https://doi.org/10.1038/s41467-019-10685-0>.
- [18] Y. Seki, T. Ishiyama, D. Sasaki, J. Abe, Y. Sohma, K. Oisaki, M. Kanai, *J. Am. Chem. Soc.* **2016**, *138*, 10798, <https://doi.org/10.1021/jacs.6b06692>.
- [19] Q. Shu, T. Kenny, J. Fan, C. J. Lyon, L. H. Cazares, T. Y. Hu, *PLoS Pathog.* **2021**, *17*, e1010039, <https://doi.org/10.1371/journal.ppat.1010039>.
- [20] A. Brik, S. Ficht, C.-H. Wong, *Curr. Opin. Chem. Biol.* **2006**, *10*, 638, <https://doi.org/10.1016/j.cbpa.2006.10.003>.
- [21] Y. Wada, M. Tajiri, S. Yoshida, *Anal. Chem.* **2004**, *76*, 6560, <https://doi.org/10.1021/ac049062o>.

#### License and Terms



This is an Open Access article under the terms of the Creative Commons Attribution License CC BY 4.0. The material may not be used for commercial purposes.

The license is subject to the CHIMIA terms and conditions: (<https://chimia.ch/chimia/about>).

The definitive version of this article is the electronic one that can be found at <https://doi.org/10.2533/chimia.2025.12>